Progress In Electromagnetics Research M, Vol. 56, 189–196, 2017

Improvement of Radiation Characteristics of Balanced Antipodal Vivaldi Antenna Using Transformation Optics

Fatemeh Etesami[1, *], Shapur Khorshidi[1], Shaghayegh Shahcheraghi[2], and Alireza Yahaghi[2]

Abstract—Transformation optics is a convenient method to control paths of electromagnetic waves and radiation characteristics of antennas. In this paper, we try to increase the gain of Balanced Antipodal Vivaldi Antenna (BAVA) over 8–16 GHz frequency band using an optical conformal transformation. The proposed antenna can be implemented by ordinary dielectric materials and graded photonic crystals (GPCs). In this designed BAVA, better side-lobe level (SLL) and cross-polarization are achieved compared to a conventional BAVA. Simulation results validate the performance of the design approach.

1. INTRODUCTION

Ultra-wideband (UWB) communication systems have the promise of very high bandwidth, reduced fading from multipath and low power requirements. Advancement in these kinds of systems necessitates UWB, multifunctional and compact antennas [1]. Vivaldi antenna is a travelling wave, end fire and planar antenna which has been utilized in many ultra wideband (UWB) applications, such as ground penetrating radars, radio astronomy, and UWB imaging systems [2, 3]. Vivaldi antenna was originally introduced by Gibson in 1979 [4] and was significantly improved in terms of bandwidth and cross polarization applying a balanced antipodal structure by Langley et al. in 1993 [5]. Many techniques have been used to alter the radiation characteristics of the antenna [1, 3, 6, 7]. Double-slot Vivaldi antenna (DSVA) and balanced antipodal Vivaldi antenna with a director in its aperture are used to enhance the directivity of the antenna [3, 7]. By applying a dielectric lens in front of the antenna's aperture, the beam-tilting in the E-plane was improved within the operation bandwidth [8]. The bandwidth of Vivaldi antenna can also be improved by modification of radiating fins [1].

Transformation optics (TO) is a new approach to the design of electromagnetic structures and was introduced by Pendry et al. [9] and Leonhardt [10] in 2006. In this method, the paths of electromagnetic waves inside a material are controlled by introducing a prescribed spatial variation in the constitutive parameters (the electric permittivity and magnetic permeability) [11]. As an interesting application, for example, using this powerful method can improve the radiation characteristics of the antenna [13, 14]. TO relies on the form-invariance of Maxwell's equations under a spatial coordinate transformation [10, 12]. This design procedure (using TO) usually leads to non-isotropic materials whose implementation is complicated. Metamaterials are a prominent candidate for realizing these complex materials, however, usually suffer from limited operation bandwidth and intrinsic losses [13]. It may be possible to achieve a simpler medium by limiting the transformation to the cases satisfying Cauchy-Riemann equations [13, 14], in which, the transformation is called conformal [10, 12, 15]. Using this method, the obtained material can be realized by natural dielectrics, and therefore, the problems regarding the difficult implementation, narrow bandwidth and intrinsic losses are solved [12].

Received 31 January 2017, Accepted 27 April 2017, Scheduled 10 May 2017

* Corresponding author: Fatemeh Etesami (Etesami.shirazu@gmail.com).

[1] Air Ocean Complex, Malek-Ashtar University of Technology, Shiraz, Iran. [2] School of Electrical and Computer Engineering, College of Engineering, Shiraz University, Shiraz, Iran.

By applying the mentioned technique to the balanced antipodal Vivaldi antenna, one can control the paths of electromagnetic waves and improve the antenna performance.

In this paper, an improved compact balanced antipodal Vivaldi antenna (BAVA) is designed and realized by using conformal transformation optics. For implementation of the resultant media, a graded photonic crystal (GPC) is utilized as the substrate. The designed antenna operates over 8–16 GHz band. These structural modifications are employed to improve the gain, side-lobe levels (SLLs) and cross-polarization of conventional BAVA. Section 2 describes the design methodology of the antenna, and Section 3 outlines the simulated results.

2. DESIGN METHOLOGY

Converting spherical wavefront to planar one in the aperture of the antenna can increase its gain [14]. Optical conformal transformation is employed to realize this idea. The main advantage of conformal mapping is that the obtained media will be isotropic and can be implemented by graded refractive index (GRIN) materials [13].

Figure 1 illustrates the geometry and parameter values of the copper pattern of a typical BAVA. Different curvatures of the antenna can be derived by the following exponential function [7]

$$z = \pm A \times e^{P(x-B)} + C \tag{1}$$

where A, B, C and P are constant numbers defined for three curvatures E_t, E_f and E_a of the antenna according to Table 1. RT/duroid 6002 is selected as the base dielectric substrate of the antenna with relative permittivity equal to 2.94 and dielectric loss tangent equal to 0.0012.

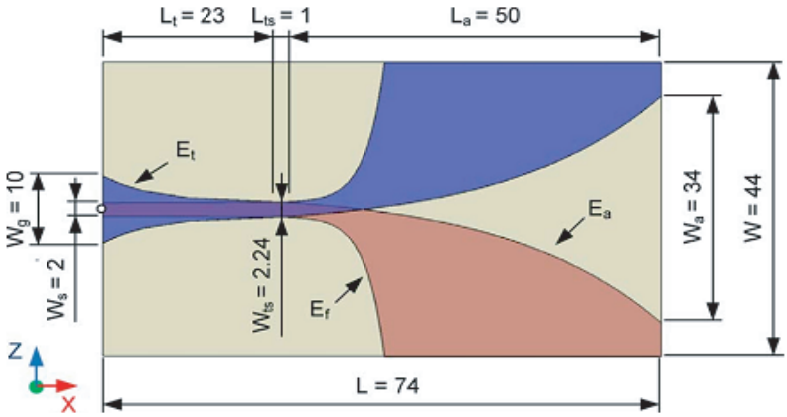

Figure 1. Geometry of the BAVA [7].

Table 1. Curvatures parameters of antenna in Fig. 1 [7].

Curves	Parameters			
	$A_{t,f,a}$	$P_{t,f,a}$	$B_{t,f,a}$	$C_{t,f,a}$
E_t	$\frac{W_{ts}-W_g}{2\times(e^{(P_t\times L_t)}-1)}$	-0.15	0	$\frac{W_g}{2} - A_t$
E_f	0.1	0.4	$L_t + L_{ts}$	$\frac{W_{ta}}{2} - A_f$
E_a	$\frac{W_{ts}-W_a}{2\times(e^{(P_a\times L_a)}-1)}$	0.05	$L_t + L_{ts}$	$-\frac{W_{ts}}{2} - A_a$

An exploded view of the original BAVA construction is plotted in Fig. 2. It consists of three copper layers; the two external layers are the ground planes, and the central layer is the conductor. The copper layers are separated by two dielectric substrates [7].

The optimized transformation can be exactly conformal if the physical and virtual spaces have the same conformal module [14]. For designing the desired media using GRIN materials, we consider

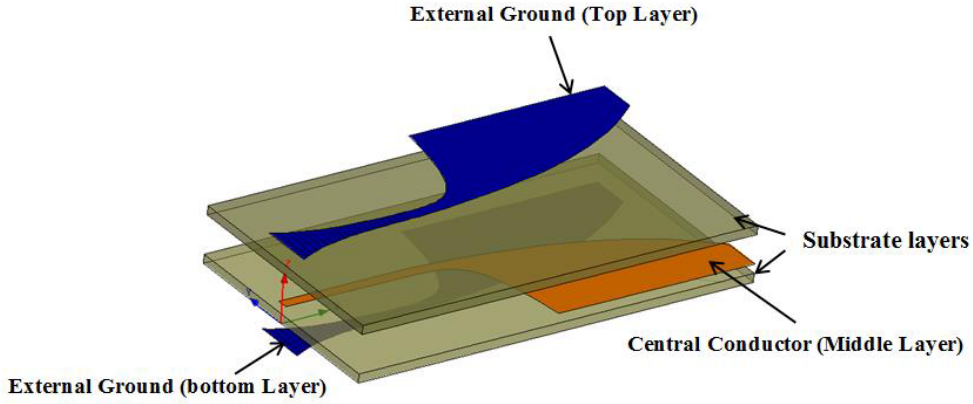

Figure 2. Exploded view of the BAVA construction.

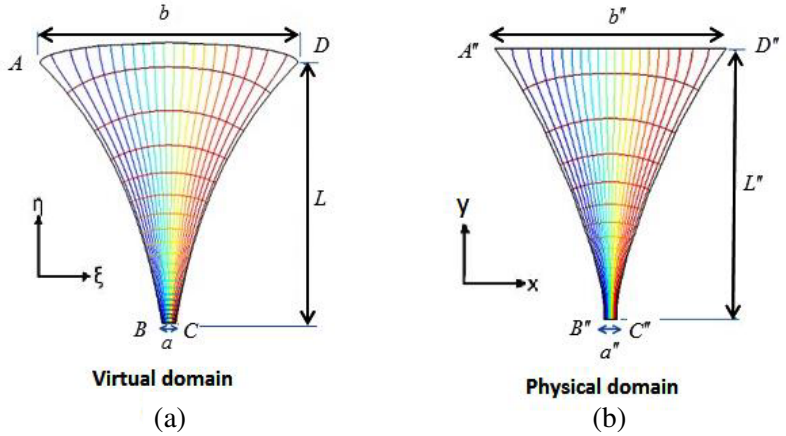

Figure 3. Process of conformal mapping. (a) Virtual domain, (b) physical domain.

Fig. 3(a) in which $a = 1.7\,\text{mm}$, $b = 34\,\text{mm}$ and $L = 34\,\text{mm}$ as virtual space. This figure is mapped conformally to a physical region shown in Fig. 3(b) which is the desired domain with flattened wavefront with $a'' = 1.7\,\text{mm}$, $b'' = 30\,\text{mm}$ and $L'' = 34.6\,\text{mm}$. The values of b'' and L'' have been selected so that the conformal modules (M) of the Vivaldi antenna in both virtual and physical spaces are almost the same. The conformal module is obtained by $M = (1/a)(\int_{AB} |\partial u/\partial n| ds)$ where u is the first coordinate of the intermediate Cartesian mapping space, and the vector $\hat{n}$ is the outward normal to the boundary [13]. In order to simplify the mapping from virtual space to physical space, a rectangular shape with the same conformal module (M) is considered as an intermediate region. Using the feature that only one parameter varies along each boundary, determination of the conformal mapping is reduced to solving Laplace's equations subject to classical Dirichlet and/or Neumann boundary conditions by a normal PDE solver [14].

For Cartesian coordinates in the virtual, intermediate and physical space, the notations (ξ, η), (u, v) and (x, y) are used, respectively. The details of the utilized mapping and corresponding equations are explained in [13] and [14]. Refractive index in the intermediate space $(n'(u, v))$ is calculated by interpolation of the obtained refractive index in the virtual domain $(n'(\xi, \eta))$. By calculating $u(x, y)$ and $v(x, y)$ through solving Laplace's equations in the intermediate space and knowing the material properties of the intermediate domain $(n'(u, v))$, the refractive index in the physical space is obtained by [13]:

$$n(x, y) = n'(u, v) \times \left[\left(\frac{\partial u}{\partial x} \right)^2 + \left(\frac{\partial u}{\partial y} \right)^2 \right] \tag{2}$$

COMSOL Multiphysics is used to solve the required Laplace's equations. The distribution of the obtained relative permittivity in the physical space is presented in Fig. 4 which varies between 0.0277 and 2.6658. Therefore, the obtained material is a dispersive one. Permittivity values less than unity can be implemented using metamaterials. However, due to their resonant structures, the frequency bandwidth is usually limited. To overcome this problem, all values smaller than 1 are replaced with 1, which have no impact on the antenna performance because its region is very small.

The obtained antenna can now be implemented by both ordinary dielectrics and isotropic graded refractive index (GRIN) materials [12]. In this work, the second method is used. This technique is realized by graded photonic crystals (GPCs) operating in metamaterial regime. GPCs indeed consist of dielectric rods with varying radii. In order to implement the designed media, in the first step, the continuous distribution of the refractive index is discretized using a square-cell network. In this form, ij-cell of the network is a square with side $d = 0.9\,\text{mm}$, and n_{ij} is the refractive index at the point (x_i, y_j). Then an array of air holes is drilled into the original substrate of the antenna ($\varepsilon_{rod} = 1$ and

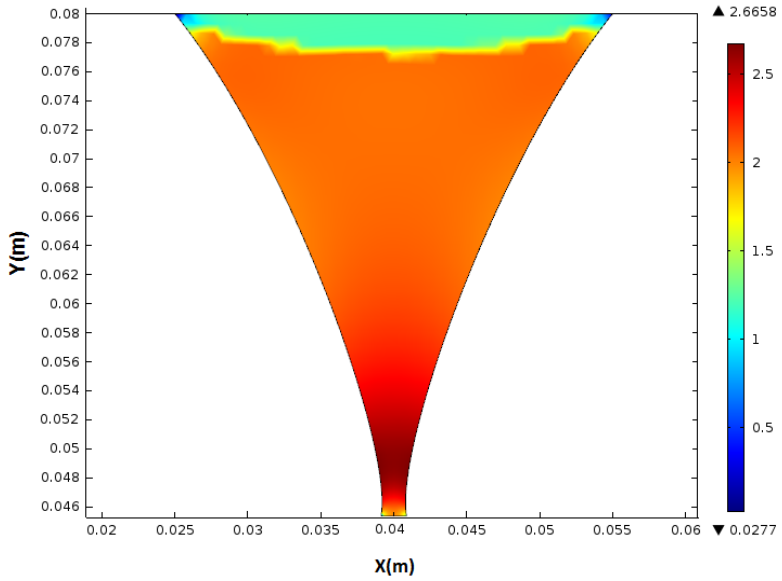

Figure 4. Profile of the relative permittivity for the proposed antenna (at 10 GHz).

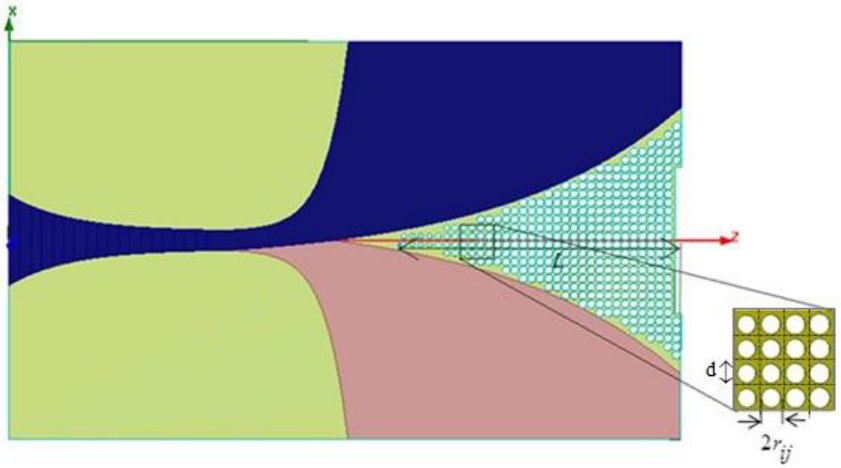

Figure 5. Implementation of the refractive index profile with the graded photonic crystals.

$\varepsilon_{host} = 2.94$). For TM polarization, the rods radii can be calculated using [16]:

$$r_{ij} = d\sqrt{\frac{\left(\varepsilon_{host} - n_{ij}^2\right)\left(\varepsilon_{host} + \varepsilon_{rod}\right)}{\pi\left(\varepsilon_{host} + n_{ij}^2\right)\left(\varepsilon_{host} - \varepsilon_{rod}\right)}} \tag{3}$$

A scheme of the obtained holes in the antenna's substrate is shown in Fig. 5. As observed, for having better matching between drilling substrate and air, a thin row of substrate is cut. It should be noted that the dimensions of the designed antenna are the same as those of the conventional antenna indicated in Fig. 1.

If the designed media are placed in the original antenna, the spherical waves of the antenna are transformed to plane waves through propagating inside the antenna (Fig. 6). This leads to increase of the directivity in the antenna.

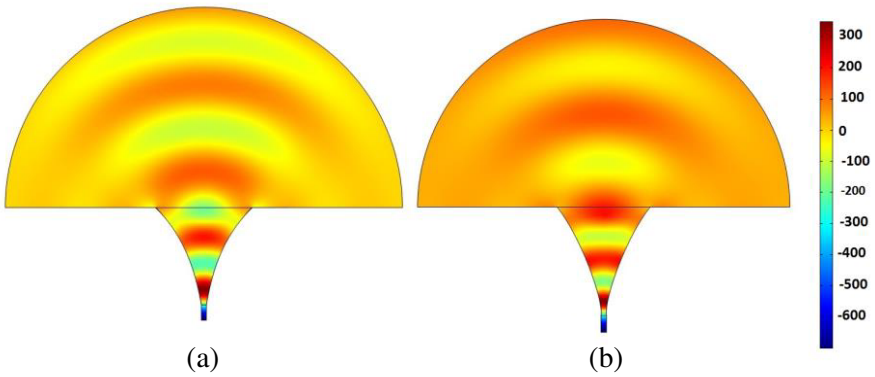

Figure 6. Distribution of the electric field (E_x) inside and outside of the antenna at $f = 10\,\text{GHz}$ for (a) conventional BAVA and (b) the GPC-based designed BAVA.

3. SIMULATION RESULTS

In this section, we demonstrate simulation results of the designed BAVA and conventional BAVA including return loss, gain, radiation pattern, side-lobe level and cross-polarization obtained of commercial simulation software CST.

Figure 7 shows the return loss of the conventional BAVA and proposed BAVA. The operating frequency band of both antennas is even more than the required operating frequency band (8–16 GHz), and they lie in the category of ultra wideband (UWB) antennas.

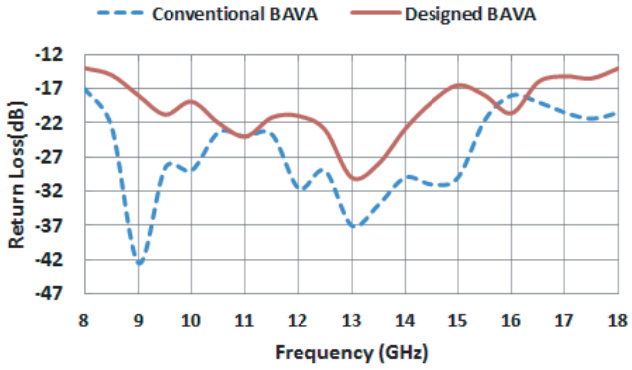

Figure 7. Simulated return loss for conventional BAVA and the proposed BAVA.

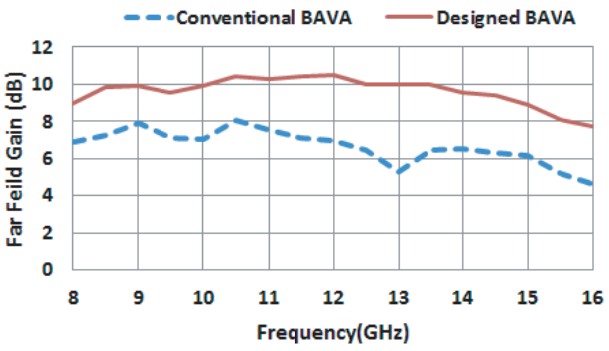

Figure 8. Far field gain of conventional and the designed BAVA.

Figure 8 shows the far-field gain for both conventional and designed BAVAs. Results imply that the gain improvement is about 2.01–4.66 dB in the entire frequency band.

Radiation patterns of the conventional BAVA and proposed BAVA at 8, 9, 10, 12, 14 and 16 GHz are plotted in Fig. 9. Simulation results indicate enhancement in gain and reduction of side-lobe levels especially in the beginning of the operating frequency band for the designed BAVA compared to the conventional BAVA. Implementation of the obtained continuous relative permittivity by isotropic graded refractive index (GRIN) materials is based on the assumption of having unit cells much smaller than the wavelength. Therefore, the efficiency of the designed antenna is deteriorated as frequency increases.

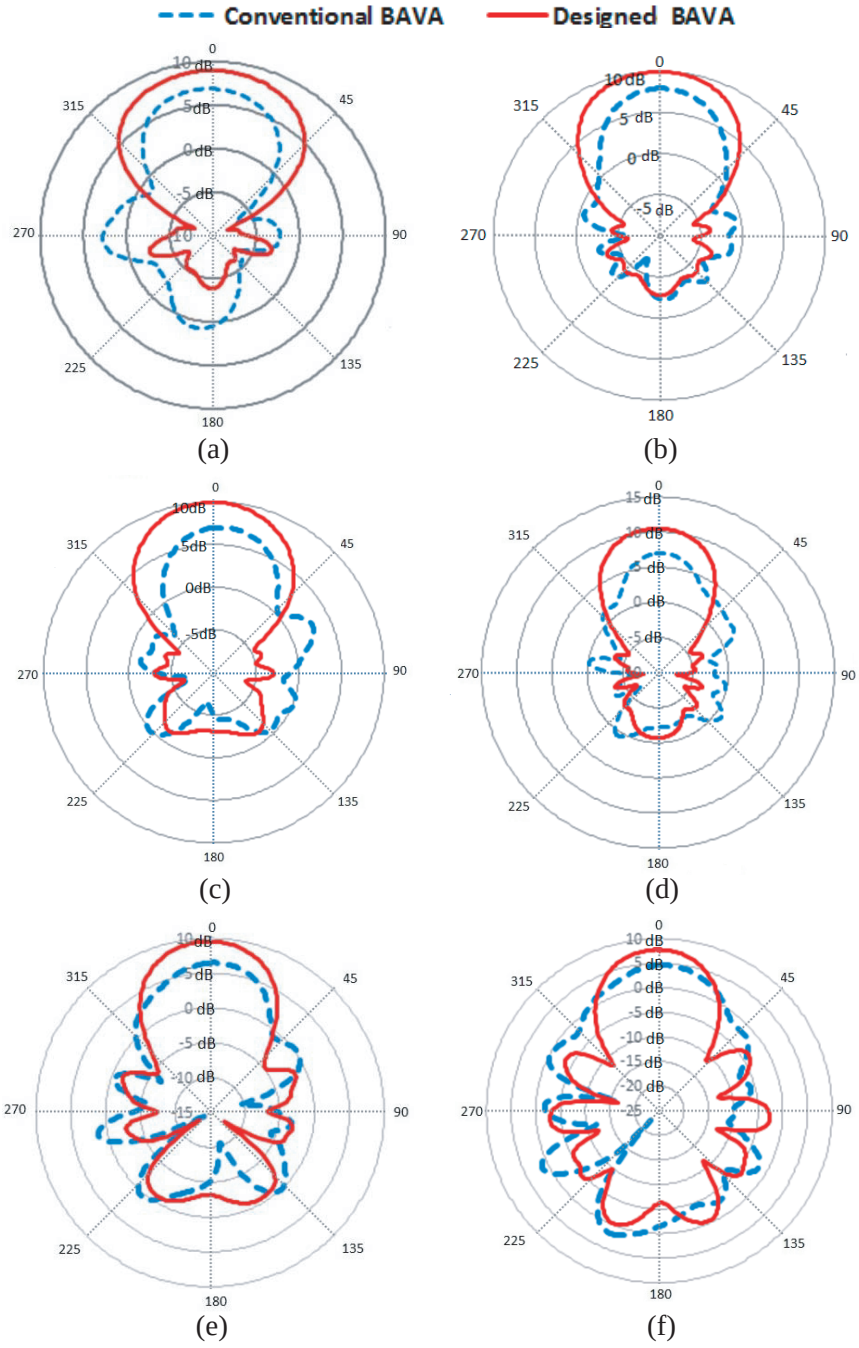

Figure 9. *E*-plane radiation patterns of the conventional BAVA and designed BAVA at (a) 8 GHz, (b) 9 GHz, (c) 10 GHz, (d) 12 GHz, (e) 14 GHz, (f) 16 GHz.

As can be seen from Fig. 6, using conformal TO leads to smoother variation of the electric field distribution. This in turn reduces the side lobe levels of the antenna. Fig. 10 compares the side-lobe levels of the proposed BAVA and the conventional BAVA at the entire operation frequency band. It can be observed that the improvement of the side-lobe levels is about 1.6–7.3 dB in the designed BAVA compared to the conventional one.

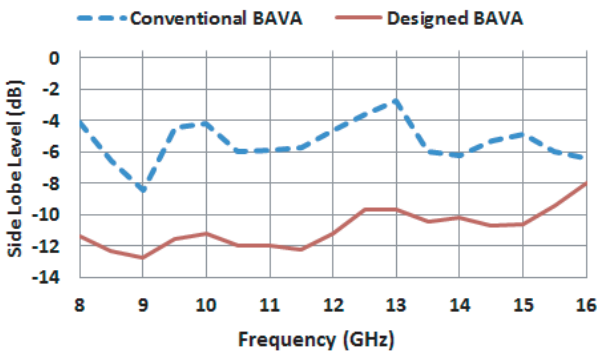

Figure 10. Side lobe levels of conventional and the proposed BAVA.

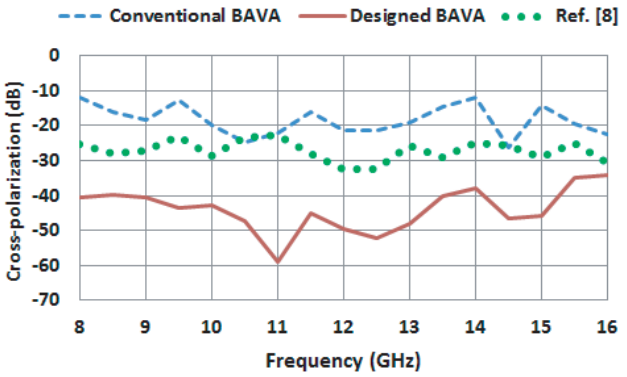

Figure 11. Cross-polarization of E-plane for the designed BAVA, conventional BAVA and lens BAVA [8].

In addition to the gain and side-lobe level, the cross-polarization of the antenna has also been improved by applying TO. Fig. 11 presents the cross-polarization of the designed BAVA and compares it with the conventional BAVA and lens BAVA [8]. It can be seen that the designed antenna has lower cross-polarization level than the other two antennas in the entire frequency band. In fact, converting spherical wavefront to planar one in the aperture of the antenna leads to decrease of the electric field component that produces the cross polarization.

A quantitative comparison of the far-field gain, side-lobe levels and cross polarization for the designed antenna and proposed antennas in [6] and [8] is presented in Table 2. It is seen that the lens BAVA in [8] can provide better gain. However, our proposed antenna has less cross polarization than two other antennas. Side-lobe level values are not mentioned in [6] and [8].

Table 2. Far field gain, cross polarization and side lobe level.

Parameter	Designed BAVA	Ref. [6]	Ref. [8]
Maximum gain, dB	10.5	9.3	13
Cross polarization, dB (average on band)	−43.9	−25	−27
Side lobe level, dB (average on band)	−10.89	-	-

4. CONCLUSION

In this paper, we propose a new BAVA with improved gain and side-lobe levels over 8–16 GHz by applying the advanced conformal transformation optics. This technique leads to utilization of homogeneous isotropic nonmagnetic material. The maximum improvement of 4.3 dB for the gain is obtained in 13 GHz. The increase of the gain is achieved by converting spherical wavefront in antenna aperture to planar one. The side-lobe level improvement is about 1.6–7.3 dB in the entire frequency band. For the design implementation, graded photonic crystals having wide bandwidth and low losses are used. By applying TO, in addition to the gain and side-lobe levels, the cross polarization is also improved to about 44 dB. The simulation results show more than 66% bandwidth for the designed BAVA; therefore, the new BAVA meets the requirements of an UWB antenna.

REFERENCES

1. Natarajan, R., J. V. George, M. Kanagasabai, and A. Kumar Shrivastav, "A compact antipodal vivaldi antenna for UWB applications," *IEEE Antennas and Wireless Propagation Letters*, Vol. 14, 1557–1560, 2015.
2. Milligan, T. A., *Modern Antenna Design*, 2nd Edition, Wiley Interscience, IEEE Press, 2005.
3. Wang, Y. W., G. M. Wang, and B. F. Zong, "Directivity Improvement Of Vivaldi Antenna Using Double-Slot Structure," *IEEE Antennas and Wireless Propagation Letters*, Vol. 12, 2013.
4. Gibson, P. J., "The Vivaldi aerial," *Microwave Conference*, 101–105, 1979.
5. Langley, J., P. Hall, and P. Newham, "Novel ultrawide-bandwidth Vivaldi antenna with low crosspolarisation," *Electronics Lett.*, Vol. 29, No. 23, 2004–2005, 1993.
6. Langley, J. D. S., P. S. Hall, and P. Newham, "Balanced antipodal Vivaldi antenna for wide bandwidth phased arrays," *IEE Proc. — MMOW Antennas Propag.*, Vol. 143, No. 2, April 1996.
7. Bourqui, J., M. Okoniewski, and E. C. Fear, "Balanced antipodal Vivaldi antenna with dielectric director for near-field microwave imaging," *IEEE Trans. Antennas and Propagation*, Vol. 58, No. 7, 2318–2326, 2010.
8. Molaei, A., M. Kaboli, S. A. Mirtaheri, and M. S. Abrishamian, "Dielectric lens balanced antipodal Vivaldi antenna with low cross-polarisation for ultra-wideband applications," *IET Microwaves, Antennas & Propagation*, Vol. 8, No. 14, 1137–1142, 2014.
9. Pendry, J. B., D. Schuring, and D. R. Smith, "Controlling electromagnetic fields," *Science*, Vol. 312, No. 5781, 1780–1782, 2006.
10. Leonhardt, U., "Optical conformal mapping," *Science*, Vol. 312, No. 5781, 1777–1780, 2006.
11. Schurig, D., J. J. Mock, B. J. Justice, S. A. Cummer, J. B. Pendry, A. F. Starr, and D. R. Smith, "Metamaterial electromagnetic cloak at microwave frequencies," *Science*, Vol. 314, No. 5801, 977–980, 2006.
12. Turpin, J. P., A. T. Massoud, Z. H. Jiang, P. L. Werner, and D. H. Werner, "Conformal mappings to achieve simple material parameters for transformation optics devices," *Optics Express*, Vol. 18, No. 1, 244–252, 2009.
13. Shahcheraghi, S. and A. Yahaghi, "Design of a pyramidal horn antenna with low E-plane sidelobes using transformation optics," *Progress In Electromagnetics Research M*, Vol. 44, 109–118, 2015.
14. Aghanejad, I., H. Abiri, and A. Yahaghi, "Design of high-gain lens antenna by gradient-index metamaterials using transformation optics," *IEEE Trans. Antennas and Propagation*, Vol. 18, No. 1, 4074–4081, 2012.
15. Landy, N. I. and W. J. Padilla, "Guiding light with conformal transformations," *Optics Express*, Vol. 17, 14872–14879, 2009.
16. Vasic, B., G. Isic, R. Gajic, and K. Hingerl, "Controlling electromagnetic fields with graded photonic crystals in metamaterial regime," *Optics Express*, Vol. 18, 20321–20333, 2010.